Mechanism of stochastic switching in single-atom absorptive bistability

Jie Wu and Hideo Mabuchi

Mechanism of stochastic switching in single-atom absorptive bistability

Jie Wu[*] and Hideo Mabuchi

E. L. Ginzton Laboratory, Stanford University, Stanford, CA 94305, USA

(Dated: June 11, 2018)

We analyze a single-atom cavity QED model to isolate the dynamic mechanism of stochastic switching between regions of state space associated with mean-field attractors of absorptive bistability. We present evidence from simulations that such switching is correlated with variations in the timings of atomic spontaneous emission events, and interpret this finding in terms of the dynamics of the coupled intracavity field and atomic dipole. Somewhat suprisingly, both upward and downward (in intracavity photon number) switching transitions may be induced by rapid succession of several atomic emissions. Based on our results we propose an implementation of bidirectional 'toggle' control for a single-atom optical latch.

I. INTRODUCTION

Cavity nonlinear optics provides a rich physical paradigm for theoretical analyses and proof-of-concept experiments in ultra-low energy all-optical switching [1–3]. Attojoule-scale switching energies can be achieved realistically in the specialized setting of cavity quantum electrodynamics (cavity QED), but in this regime of small intracavity photon numbers, quantum noise exerts a strong influence on device operation [4, 5]. One of the elementary physical phenomena enabling such logic devices is absorptive optical bistability, which has been studied extensively in the semi-classical (mean field) limit of cavity QED [6] as well as the single-atom strong-coupling quantum regime [7, 8]. Quantum noise-induced switching between metastable states has been observed in single-atom cavity QED experiments [5] with quantitative details well accounted for by first-principles theory. In the related context of dispersive optical bistability a coherent feedback strategy for suppressing quantum noise-induced switching–which represents a fundamental error process for ultra-low energy photonic logic–has been analyzed theoretically [9]. However for single-atom absorptive bistability no comparable control schemes have yet been proposed. Our aim in this paper is to develop an intuitive understanding of the quantum dynamics of stochastic switching in order to facilitate future work in quantum control. As a first step in the latter direction we suggest a way to achieve bidirectional 'toggle' control of switching in single-atom absorptive bistability, which has no direct counterpart in the classical limit.

II. THEORETICAL MODELS

The quantum model we use is built upon the driven Jaynes-Cummings Hamiltonian [10], which models the interaction between a single mode of an optical cavity having a resonant frequency ω_c and a two-level atom with ground state $|g\rangle$, excited state $|e\rangle$ and transition

frequency ω_a. For an atom-field coupling constant g and an external coherent driving field with frequency ω_l and amplitude $\mathcal{E}$ (by properly choosing the time origin we can assume $\mathcal{E}$ is real) coupled to the cavity mode, the Hamiltonian in the rotating wave approximation written in a frame rotating at the driving frequency ω_l is given by ($\hbar = 1$):

$$H = \Delta_c a^\dagger a + \Delta_a \sigma_+ \sigma_- + ig(a^\dagger \sigma_- - a\sigma_+) + i\mathcal{E}(a^\dagger - a) \quad (1)$$

where $\Delta_a = \omega_a - \omega_l$ and $\Delta_c = \omega_c - \omega_l$. In equation (1), a is the annihilation operator for the chosen cavity mode (which we will refer to as "cavity field" below) and $\sigma_- = |g\rangle\langle e| = (\sigma_x - i\sigma_y)/2$ is the atomic lowering operator. In addition to the coherent dynamics governed by (1) there are two dissipative channels for the system: the atom may spontaneously emit into modes other than the chosen cavity mode at a rate $2\gamma_\perp$, and photons may leak out of the cavity mirror at a rate 2κ. Assuming only these two incoherent processes the overall dynamics can be described by the following stochastic Schrödinger equation [10]:

$$i\frac{d}{dt}|\psi\rangle = H_{eff}|\psi\rangle \quad (2)$$

with the collapse operators:

$$C_1 = \sqrt{2\kappa}a \quad C_2 = \sqrt{2\gamma_\perp}\sigma_- \quad (3)$$

and the effective non-Hermitian Hamiltonian:

$$H_{eff} = H - \frac{i}{2}\sum_k C_k^\dagger C_k$$
$$= \Delta_c a^\dagger a + \Delta_a \sigma_+ \sigma_- + ig(a^\dagger \sigma_- - a\sigma_+) + i\mathcal{E}(a^\dagger - a)$$
$$- i\kappa a^\dagger a - i\gamma_\perp \sigma_+ \sigma_- \quad (4)$$

The continuous evolution of the stochastic Schrödinger equation (2) is interrupted by quantum jumps in which the state vector $|\psi\rangle$ collapses to

$$|\psi\rangle \mapsto \frac{C_k|\psi\rangle}{\|C_k|\psi\rangle\|}, \quad (5)$$

the probability of the collapse in an interval dt being given by $\|C_k|\psi\rangle\|^2 dt$. This makes the time evolution of

* bayern.science@gmail.com

$|\psi(t)\rangle$ a multidimensional stochastic process. Such a time series of $|\psi(t)\rangle$ is known as a quantum trajectory of the system evolution. The time series of $|\psi(t)\rangle$ may be used to find the trajectory for the expectation of any operator O acting on the system Hilbert space using the following formula:

$$\langle O\rangle = \frac{\langle\psi(t)|O|\psi(t)\rangle}{\langle\psi(t)|\psi(t)\rangle} \qquad (6)$$

Apart from the stochastic process perspective there is also a statistical ensemble description of the system dynamics, which is described by the following unconditional master equation [10]:

$$\dot{\rho} = -i[H,\rho] + \kappa(2a\rho a^\dagger - a^\dagger a\rho - \rho a^\dagger a) \\ + \gamma_\perp(2\sigma_-\rho\sigma_+ - \sigma_+\sigma_-\rho - \rho\sigma_+\sigma_-) \qquad (7)$$

whose density-matrix solution corresponds to the (stochastic) ensemble average of all possible quantum trajectories. The master equation (7) can also be used to find the dynamical equations for the expectation of any operator O acting on the system Hilbert space using the formula $\langle\dot{O}\rangle = \mathrm{Tr}[O\dot{\rho}]$. The simplest set of operators that can approximately describe the system state is $\{a, \sigma_-, \sigma_z\}$. Applying the above trace formula we obtain:

$$\langle\dot{a}\rangle = -(\kappa + i\Delta_c)\langle a\rangle + g\langle\sigma_-\rangle + \mathcal{E} \\ \langle\dot{\sigma_-}\rangle = -(\gamma_\perp + i\Delta_a)\langle\sigma_-\rangle + g\langle a\sigma_z\rangle \\ \langle\dot{\sigma_z}\rangle = -2\gamma_\perp(1 + \langle\sigma_z\rangle) - 2g(\langle a^\dagger\sigma_-\rangle + \langle a\sigma_+\rangle) \qquad (8)$$

The above operator expectation equations (8) also apply to the case of N non-interacting atoms each coupled to the same cavity mode with the same coupling constant g. In this case the atomic operators are the sums of those of individual atoms [8]:

$$\sigma_- = \sum_{j=1}^N \sigma_-^j, \quad \sigma_z = \sum_{j=1}^N \sigma_z^j \qquad (9)$$

Note that the moment evolution equations (8) are not closed as they contain expectations of operator products. A common practice in the quantum optics community to close the equations is to simply factorize the operator products, e.g. $\langle a^\dagger\sigma_-\rangle \approx \langle a^\dagger\rangle\langle\sigma_-\rangle$, which corresponds to taking the thermodynamic limit of many weakly excited atoms hence the correlations between the atomic operators and the field operator average to zero [6, 7] (see also [11, 12] for alternative derivations). The closed equations after factorization are the well-known Maxwell-Bloch Equations (MBEs):

$$\langle\dot{a}\rangle = -(\kappa + i\Delta_c)\langle a\rangle + g\langle\sigma_-\rangle + \mathcal{E} \\ \langle\dot{\sigma_-}\rangle = -(\gamma_\perp + i\Delta_a)\langle\sigma_-\rangle + g\langle a\rangle\langle\sigma_z\rangle \\ \langle\dot{\sigma_z}\rangle = -2\gamma_\perp(1 + \langle\sigma_z\rangle) - 2g(\langle a^\dagger\rangle\langle\sigma_-\rangle + \langle a\rangle\langle\sigma_+\rangle) \qquad (10)$$

Under the resonance condition $\Delta_c = \Delta_a = 0$ (we will always assume this resonance condition in the following)

$\langle a\rangle$ and $\langle\sigma_-\rangle$ are real thus the above MBEs can be rewritten using the following physical observables: cavity field amplitude quadrature $x = (a + a^\dagger)/2$, and Pauli matrices $\sigma_x = (\sigma_+ + \sigma_-)$ and σ_z

$$\langle\dot{x}\rangle = -\kappa\langle x\rangle + \frac{g}{2}\langle\sigma_x\rangle + \mathcal{E} \\ \langle\dot{\sigma_x}\rangle = -\gamma_\perp\langle\sigma_x\rangle + g\langle x\rangle\langle\sigma_z\rangle \\ \langle\dot{\sigma_z}\rangle = -2\gamma_\perp(1 + \langle\sigma_z\rangle) - 2g\langle x\rangle\langle\sigma_x\rangle \qquad (11)$$

To visualize the atom-field interaction it is useful to rewrite the driving terms of the atomic operator expectation equations in the form of the classical equation of motion for a magnetic moment in a static magnetic field:

$$\frac{d}{dt}\begin{pmatrix}\langle\sigma_x\rangle\\0\\\langle\sigma_z\rangle\end{pmatrix} = \frac{d}{dt}\vec{S} = 2g\vec{S}\times\vec{B} = 2g\begin{pmatrix}\langle\sigma_x\rangle\\0\\\langle\sigma_z\rangle\end{pmatrix}\times\begin{pmatrix}0\\-\langle x\rangle\\0\end{pmatrix} \qquad (12)$$

where $\vec{S} = \begin{pmatrix}\langle\sigma_x\rangle & 0 & \langle\sigma_z\rangle\end{pmatrix}^T$, $\vec{B} = \begin{pmatrix}0 & -\langle x\rangle & 0\end{pmatrix}^T$. It shows that the atomic pseudospin undergoes precession in xz-plane driven by the cavity field acting as a pseudo-magnetic field. This spin precession representation of the atomic dynamics provides a useful intuitive picture for deciphering the mechanism of stochastic switching in single-atom absorptive bistability.

III. STOCHASTIC SWITCHING INDUCED BY ATOMIC SPONTANEOUS EMISSION

Stochastic switching refers to the following phenomenon: for an absorptive bistable parameter set identified by the Maxwell-Bloch equations the quantum trajectory simulation would show that the system has two preferred states with low and high field amplitude respectively resembling absorptive bistability; however unlike in the limiting case described by the Maxwell-Bloch equations the system does not stay in one of the two states forever; instead it frequently jumps between them as is illustrated in Fig. 1 below. This observation has been confirmed by our recent experiment [5].

Since the automatic switching is a stochastic process, to search for the underlying physical mechanism we should obviously focus on the stochastic processes contained in our theoretical model, which are the atomic spontaneous emission and photon leakage out of the cavity mirror. It is intuitive that intrinsic field fluctuation due to photon leakage could induce transitions between the two metastable states as is suggested by the dispersive bistability in a Kerr-nonlinear cavity [9]. However it is not clear whether the atomic spontaneous emission also contributes to the automatic switching and if yes how it operates.

The numerical evidence for the active role of the atomic spontaneous emission in inducing the switching is based on the quantum trajectory simulation defined above [10]. In particular we used the quantum optics toolbox [13]
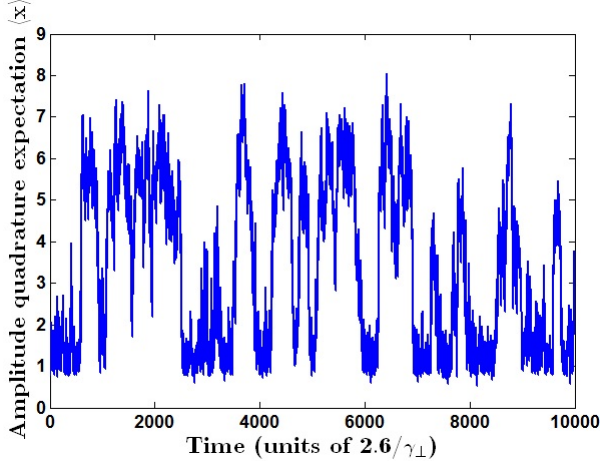
FIG. 1. A typical quantum trajectory simulation result for the evolution of the field amplitude quadrature expectation $\langle x \rangle$ for an absorptive bistable parameter set identified by the Maxwell-Bloch equations

to generate quantum trajectories. We then used 3-state Hidden Markov Model (HMM) to classify all the data points of the trajectory into 3 groups: (1) low-intensity state points (2) in-transit points and (3) high-intensity state points based on the corresponding observable expectation triplet $(\langle x \rangle, \langle \sigma_x \rangle, \langle \sigma_z \rangle)$ and defined the occurrence of switching as the moment at which the system goes from low/high-intensity state to in-transit state followed by the system going from in-transit state to high/low-intensity state and staying in the destination state for a reasonably long time. With this we collected the statistics of spontaneous emission, photon leakage and the observable expectation triplet conditioned upon the occurrence of switching using a counting window with a suitable width. Moreover we slid the counting window from the occurrence of switching backward in time just like rewinding the film to see what happened that precedes the switching. The conditioned statistics against the time the counting window is positioned for low-to-high transitions are plotted in Fig. 2 below. As we can see from the plot, there is excessive spontaneous emission preceding the onset of low-to-high transitions.

This excessive spontaneous emission is also observed in the statistics conditioned upon high-to-low transitions as is shown in Fig. 3 below.

It seems like excessive spontaneous emission is a precursor to the automatic switching. More careful examination of the effect of spontaneous emission on the above-mentioned atomic pseudospin precession reveals that excessive spontaneous emission is not just a precursor to the automatic switching but actually responsible for inducing the switching by weakening or strengthening, depending on whether the speed of precession is slow or fast, the dipole moment hence the dipole radiation that destructively interferes with the external field coupled into the cavity.
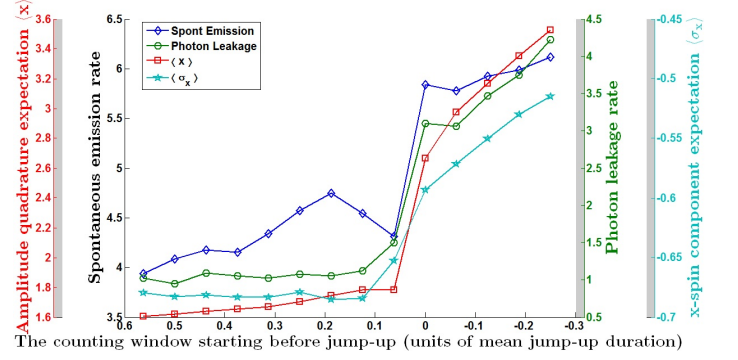

FIG. 2. The statistics of spontaneous emission, photon leakage and $\langle x \rangle, \langle \sigma_x \rangle$ conditioned upon low-to-high state transitions, where the origin of the x-axis is defined as the moment the system goes from low-intensity to in-transit state and the position of the counting window is defined as the moment we start counting; the time unit of the x-axis is chosen to be the mean time the system takes to complete the low-to-high state transitions (termed "mean jump-up duration" in the plot) and the counting window width is set to be 1/16 of the time unit
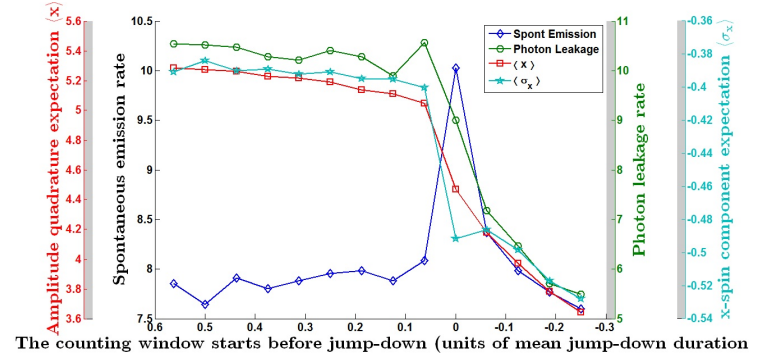

FIG. 3. The statistics of spontaneous emission, photon leakage and $\langle x \rangle, \langle \sigma_x \rangle$ conditioned upon high-to-low state transitions, where the origin of the x-axis is defined as the moment the system goes from high-intensity to in-transit state and the position of the counting window is defined as the moment we start counting; the time unit of the x-axis is chosen to be the mean time the system takes to complete the high-to-low state transitions (termed "mean jump-down duration" in the plot) and the counting window width is set to be 1/16 of the time unit

Whenever a spontaneous emission occurs the atomic pseudospin is reset to pointing vertically downward in the Bloch sphere ($\langle \sigma_z \rangle = -1$) and the dipole moment is reset to zero ($\langle \sigma_x \rangle = 0$ and recall that we are considering the resonant case thus $\langle \sigma_y \rangle \equiv 0$). After the emission, the atomic pseudospin continues precessing and because of the out of phase relation between the cavity field and the dipole moment, the cavity field drives the pseudospin back towards its position before the occurrence of spontaneous emission i.e. the dipole moment recovers. Fig. 4 below helps to visualize the consequence of spontaneous emission on the atomic pseudospin precession.
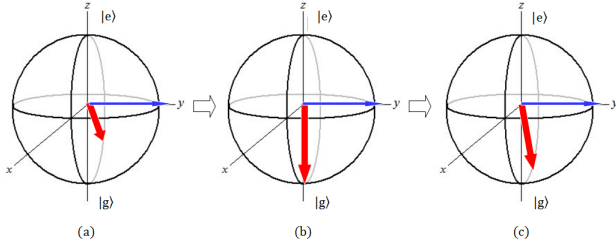
FIG. 4. Graphical representation of spontaneous emission interrupting the atomic pseudospin precession in which the thick red arrow represents the atomic pseudospin whereas the thin blue arrow represents the cavity field acting as a pseudo-magnetic field. (a) $\langle \sigma_x \rangle$ undergoes rotation mediated by $\langle x \rangle$ before spontaneous emission. (b) $\langle \sigma_x \rangle$ is reset to zero upon spontaneous emission. (c) $\langle \sigma_x \rangle$ recovers via the rotation mediated by $\langle x \rangle$ after spontaneous emission.

Therefore at low-intensity state the cavity field is weak thus the speed of precession is slow hence the recovery is slow. But once the dipole moment is recovered it will remain strong for a long time because it produces strong dipole radiation that reduces the cavity field and hence the speed of precession. As a result excessive spontaneous emission leads to weaker dipole moment and dipole radiation as is illustrated by Fig. 5 below.
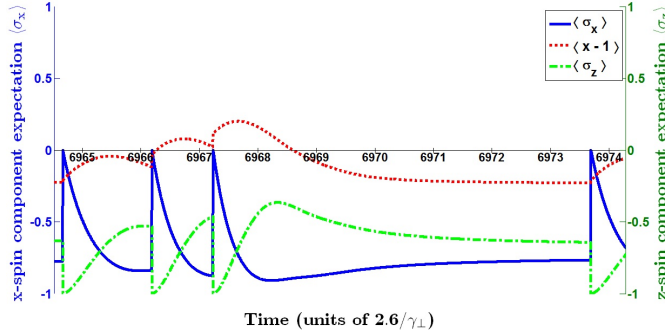

FIG. 5. Illustration of excessive spontaneous emission weakening the dipole moment when the speed of the atomic pseudospin precession is slow

In contrast, at high-intensity state the cavity field is strong thus the speed of precession is fast therefore the recovery is immediate. But once the dipole moment is recovered it will quickly precess to the opposite sign and complete many revolutions if there is no spontaneous emission to interrupt the cycling. As a consequence the dipole moment averages to almost zero when there are few emissions. This is illustrated in Fig. 6 below.

As a verification for the above hypothesis we randomly chose a trajectory and divided it into time segments of equal length and for each segment we counted the number of spontaneous emissions. After that we evaluated for each segment the time average of $\langle x \rangle$ and classified a segment as low-intensity segment if its $\langle x \rangle$ average is smaller than a chosen limit or high-intensity segment if
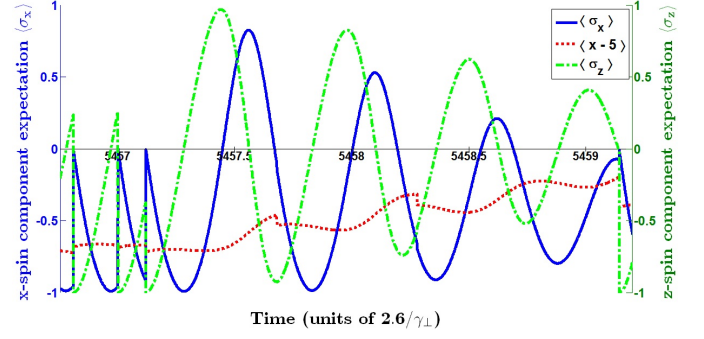

FIG. 6. Illustration of excessive spontaneous emission strengthening the dipole moment when the speed of the atomic pseudospin precession is fast

its $\langle x \rangle$ average is greater than a chosen limit. The final step consists of making a histogram for both the set of low-intensity segments and that of high-intensity segments based on the number of spontaneous emissions occurred within the segment, and evaluating for each of the histogram bins the average of $\langle \sigma_x \rangle$. The resulted histogram on the bin average of $\langle \sigma_x \rangle$ versus the number of spontaneous emissions for both the low-intensity segments and the high-intensity segments are plotted in Fig. 7 and Fig. 8 below, which show clearly the dipole moment weakening/strengthening by excessive spontaneous emission.
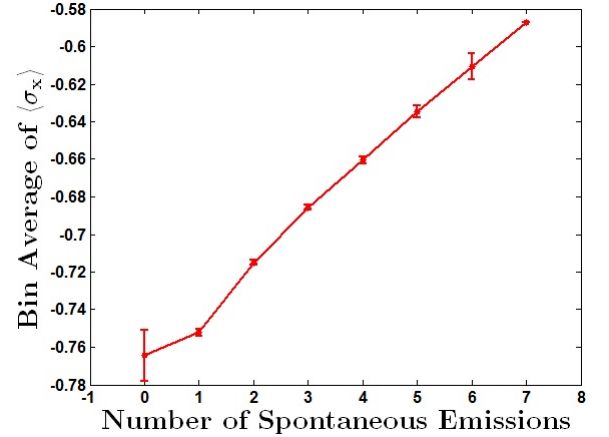

FIG. 7. Bin average of $\langle \sigma_x \rangle$ vs. the number of spontaneous emissions histogram for the low-intensity segments

IV. FLIP-FLOP CONTROL VIA SPONTANEOUS EMISSION ENHANCEMENT

With the above understanding of the switching mechanism via spontaneous emission, we proposed an implementation of flip-flop control in the context of single-atom cavity quantum electrodynamics via spontaneous emission enhancement, which provides further corroboration to the above hypothesized mechanism. The idea
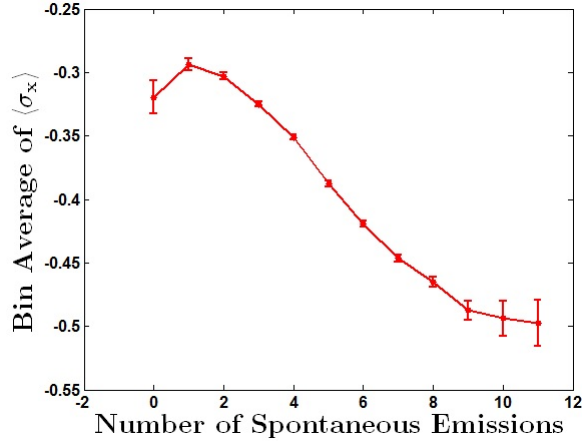
FIG. 8. Bin average of $\langle \sigma_x \rangle$ vs. the number of spontaneous emissions histogram for the high-intensity segments

is straightforward: if excessive spontaneous emission can lead to state transitions then when a state transition is desired what we need to do is just to artificially introduce excessive spontaneous emission, and there is a well-known method to enhance spontaneous emission—the Purcell effect [14]. Thus suppose we have some means to alter the cavity detuning (w.r.t. the atomic resonance frequency)—either by some kind of electro-optic mechanism or by Kerr effect with a control beam—then we can realize state transition in the first cavity, the absorptive bistable cavity, by reducing to zero the detuning of the second cavity, the cavity for spontaneous emission enhancement (which we can call the Purcell cavity). The schematic of such a flip-flip is given in Fig. 9. Fig. 10 and Fig. 11 below illustrate the flip-flop control via turning off the detuning of the Purcell cavity, where the detunings are chosen such that the effective decay rates are almost the same as the spontaneous emission rate $2\gamma_\perp$.
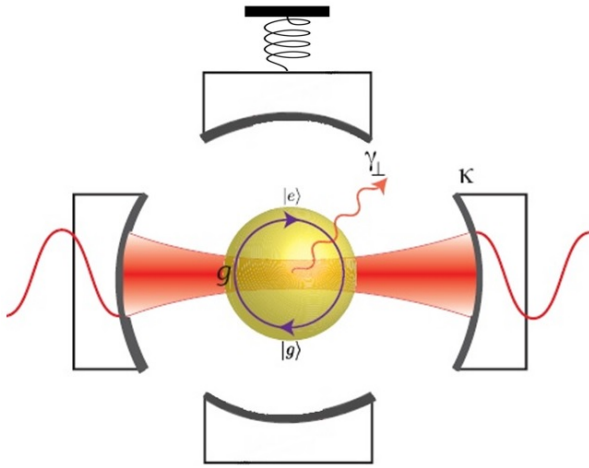

FIG. 9. A schematic of a two-cavity optical flip-flop consisting of an absorptive bistable cavity to produce the two logic states and a Purcell cavity to inducing state switching via the Purcell effect
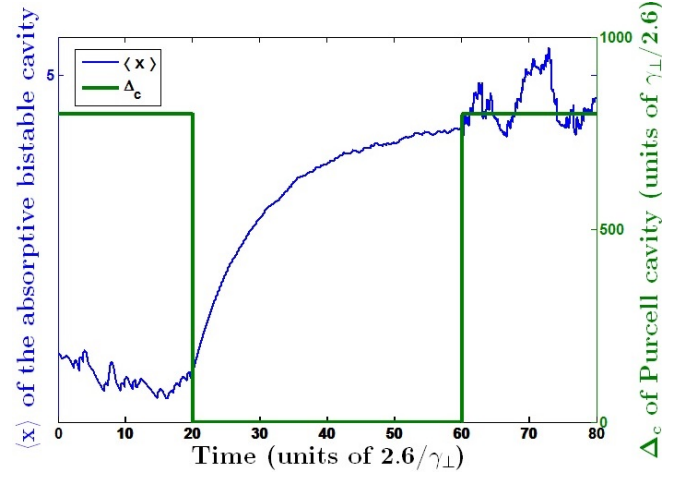

FIG. 10. Cavity enhanced spontaneous emission induces low-to-high transition in the absorptive bistable cavity by turning off the detuning of the Purcell cavity (the square-well green curve)
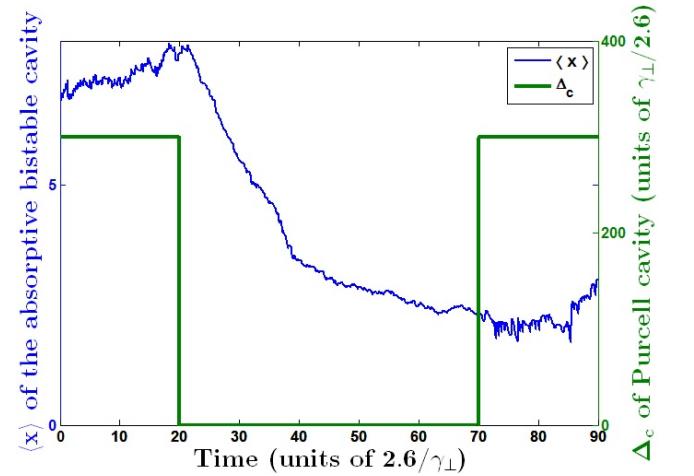

FIG. 11. Cavity enhanced spontaneous emission induces high-to-low transition in the absorptive bistable cavity by turning off the detuning of the Purcell cavity (the square-well green curve)

An added advantage of this flip-flop control is that, for conventional flip-flops the required input to trigger bit flip from "0" to "1" is different from that to trigger bit flip from "1" to "0"; however for our proposal the same input, which is turning off the detuning of the Purcell cavity, can be used to trigger both "0" to "1" and "1" to "0" bit flips.

V. SUMMARY AND CONCLUSION

In this paper we have elucidated the mechanism of excessive spontaneous emission inducing the automatic

switching between the two metastable states in the quantum analog of absorptive bistability, which is weakening or strengthening the dipole moment thus dipole radiation under weak or strong cavity field. The difference in the consequence of excessive spontaneous emission results from the difference in the speed of the atomic pseudospin precession driven by the cavity field. Based on this understanding we proposed a flip-flop control of an absorptive bistable cavity via cavity enhanced spontaneous emission using a second cavity with tunable detuning, which provides a physical basis for designing ultra-low energy optical information processing logic devices.

VI.   ACKNOWLEDGMENT

[1] H. Mabuchi, Phys. Rev. A **80**, 045802 (2009), URL http://link.aps.org/doi/10.1103/PhysRevA.80.045802.

[2] C. Santori, J. S. Pelc, R. G. Beausoleil, N. Tezak, R. Hamerly, and H. Mabuchi, Phys. Rev. Applied **1**, 054005 (2014), URL https://doi.org/10.1103/PhysRevApplied.1.054005.

[3] Y.-D. Kwon, M. A. Armen, and H. Mabuchi, Phys. Rev. Lett. **111**, 203002 (2013), URL https://doi.org/10.1103/PhysRevLett.111.203002.

[4] C. J. Hood, M. S. Chapman, T. Lynn, and H. J. Kimble, Phys. Rev. Lett. **80**, 4157 (1998), URL https://doi.org/10.1103/PhysRevLett.80.4157.

[5] J. Kerckhoff, M. A. Armen, and H. Mabuchi, Opt. Express **19**, 24468 (2011), URL https://doi.org/10.1364/OE.19.024468.

[6] L. Lugiato, Progress in Optics **21**, 69 (1984), URL http://dx.doi.org/10.1016/S0079-6638(08)70122-7.

[7] C. Savage and H. Carmichael, IEEE J. Quantum Elect. **24**, 1495 (1988), URL http://dx.doi.org/10.1109/3.7075.

[8] M. A. Armen and H. Mabuchi, Phys. Rev. A **73**, 063801 (2006), URL http://link.aps.org/doi/10.1103/PhysRevA.73.063801.

[9] H. Mabuchi, Appl. Phys. Lett. **98**, 193109 (2011), URL http://dx.doi.org/10.1063/1.3589994.

[10] H. J. Carmichael, *An Open Systems Approach to Quantum Optics* (Springer-Verlag, 1993).

[11] T. D. Ladd and Y. Yamamoto, Phys. Rev. B **84**, 235307 (2011), URL http://dx.doi.org/10.1103/PhysRevB.84.235307.

[12] H. Mabuchi, Phys. Rev. A **78**, 015801 (2008), URL https://doi.org/10.1103/PhysRevA.78.015801.

[13] T. M. Sze, J. Opt. B: Quantum and Semiclasscal Optics **1**, 424 (1999), URL http://dx.doi.org/10.1088/1464-4266/1/4/312.

[14] E. M. Purcell, Phys. Rev. **69**, 674 (1946), URL http://link.aps.org/doi/10.1103/PhysRev.69.674.2.